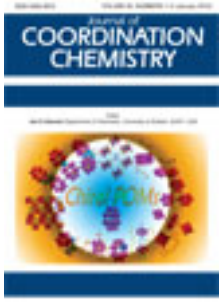

Journal of Coordination Chemistry
Publication details, including instructions for authors and subscription information:
http://www.tandfonline.com/loi/gcoo20

Synthesis, structures, and urease inhibition of nickel(II), zinc(II), and cobalt(II) complexes with similar hydroxy-rich Schiff bases

Yao Lu [a], Da-Hua Shi [b], Zhong-Lu You [a], Xiao-Shuang Zhou [a] & Kun Li [a]

[a] Department of Chemistry and Chemical Engineering, Liaoning Normal University, Huanghe Road 850#, Dalian 116029, P.R. China

[b] School of Chemical Engineering, Huaihai Institute of Technology, Lianyungang 222005, P.R. China

Published online: 20 Jan 2012.

To cite this article: Yao Lu, Da-Hua Shi, Zhong-Lu You, Xiao-Shuang Zhou & Kun Li (2012) Synthesis, structures, and urease inhibition of nickel(II), zinc(II), and cobalt(II) complexes with similar hydroxy-rich Schiff bases, Journal of Coordination Chemistry, 65:2, 339-352, DOI: 10.1080/00958972.2011.653785

To link to this article: http://dx.doi.org/10.1080/00958972.2011.653785

Journal of Coordination Chemistry
Vol. 65, No. 2, 20 January 2012, 339–352

Synthesis, structures, and urease inhibition of nickel(II), zinc(II), and cobalt(II) complexes with similar hydroxy-rich Schiff bases

YAO LU†, DA-HUA SHI‡, ZHONG-LU YOU*†, XIAO-SHUANG ZHOU† and KUN LI†

†Department of Chemistry and Chemical Engineering, Liaoning Normal University, Huanghe Road 850#, Dalian 116029, P.R. China
‡School of Chemical Engineering, Huaihai Institute of Technology, Lianyungang 222005, P.R. China

(*Received 8 August 2011; in final form 6 December 2011*)

Four new nickel(II), zinc(II), and cobalt(II) complexes, $[Zn(L^1)_2]\cdot H_2O$ (**1**), $[Ni(L^1)_2]\cdot H_2O$ (**2**), $[Ni(L^2)_2]$ (**3**), and $[Co(L^3)_2]\cdot H_2O$ (**4**), derived from hydroxy-rich Schiff bases 2-{[1-(5-chloro-2-hydroxyphenyl)methylidene]amino}-2-methylpropane-1,3-diol (HL^1), 2-{[1-(2-hydroxy-3-methoxyphenyl)methylidene]amino}-2-ethylpropane-1,3-diol (HL^2), and 2-{[1-(5-bromo-2-hydroxyphenyl)methylidene]amino}-2-methylpropane-1,3-diol (HL^3) have been synthesized and characterized by elemental analyses, infrared spectroscopy, and single-crystal X-ray determination. Each metal in the complexes is six-coordinate in a distorted octahedral coordination. The Schiff bases coordinate to the metal atoms through the imino N, phenolate O, and one hydroxyl O. In the crystal structures of HL^1 and the complexes, molecules are linked through intermolecular O–H···O hydrogen bonds, forming 1-D chains. The urease inhibitory activities of the compounds were evaluated and molecular docking study of the compounds with the *Helicobacter pylori* urease was performed.

Keywords: Schiff base; Zinc; Nickel; Cobalt; Crystal structure; Urease inhibition

1. Introduction

Considerable attention has been focused on transition metal complexes containing Schiff bases [1–4]. These complexes play an important role in coordination chemistry related to catalysis and enzymatic reactions [5, 6], magnetism and molecular architectures [7, 8]. Schiff-base complexes are of particular interest to inorganic chemists since their structural, spectral, and chemical properties often strongly depend on the detailed ligand structures. The Schiff bases 2-{[1-(5-chloro-2-hydroxyphenyl)methylidene]amino}-2-methylpropane-1,3-diol (HL^1), 2-{[1-(2-hydroxy-3-methoxyphenyl)methylidene]amino}-2-ethylpropane-1,3-diol (HL^2), and 2-{[1-(5-bromo-2-hydroxyphenyl)methylidene]amino}-2-methylpropane-1,3-diol (HL^3) (scheme 1) are similar multidentate

*Corresponding author. Email: youzhonglu@yahoo.com.cn

ISSN 0095-8972 print/ISSN 1029-0389 online
http://dx.doi.org/10.1080/00958972.2011.653785

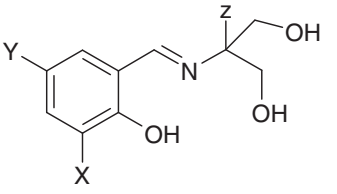

Scheme 1. The Schiff bases (for HL^1: X = H, Y = Cl, Z = Me; for HL^2: X = OMe, Y = H, Z = Et; for HL^3: X = H, Y = Br, Z = Et).

ligands, however, the complexes derived from them have seldom been reported [9–11]. Recently, we reported the urease inhibitory activity of some Schiff-base complexes [12–14]. As a detailed study on the structures and coordination behavior of the Schiff bases, and as an extension of the work on the exploration of new urease inhibitors, in this study the crystal structures and urease inhibitory activity of HL^1 and four new complexes, $[Zn(L^1)_2]\cdot H_2O$ (**1**), $[Ni(L^1)_2]\cdot H_2O$ (**2**), $[Ni(L^2)_2]$ (**3**), and $[Co(L^3)_2]\cdot H_2O$ (**4**), are investigated.

2. Experimental

2.1. *Materials and methods*

Solvents and reagents were purchased from Aldrich and used without purification. Elemental analyses for C, H, and N were performed on a Perkin-Elmer 240C elemental analyser. Infrared (IR) spectra were recorded on a Nicolet AVATAR 360 spectrometer as KBr pellets from 4000 to 400 cm^{-1}. ^1H NMR spectra were recorded on a Bruker AVANCE 500 MHz spectrometer with tetramethylsilane as internal reference. Electronic spectra were recorded on a Perkin Elmer Lambda 40 UV/Vis spectrometer using HPLC grade acetonitrile as solvent.

2.2. *Synthesis of HL^1*

To methanolic solution (20 cm^3) of 5-chlorosalicylaldehyde (0.156 g, 1.0 mmol) was added a methanolic solution (20 cm^3) of 2-amino-2-methyl-1,3-propanediol (0.105 g, 1.0 mmol) with stirring. The mixture was stirred for 20 min at room temperature to give a clear yellow solution. After keeping the solution in air for a week, yellow block-shaped crystals of HL^1, suitable for X-ray crystal structural determination, formed at the bottom of the vessel on slow evaporation of about 80% of the solvent. The crystals were isolated by filtration, washed three times with cold methanol, and dried in a vacuum desiccator using anhydrous $CaCl_2$. Yield, 0.173 g, 71%. Anal. Calcd for $C_{11}H_{14}ClNO_3$ (%): C, 54.2; H, 5.8; N, 5.8. Found: C, 54.0; H, 5.9; N, 5.7. IR data (KBr, cm^{-1}): 3316 (br, w, ν_{ArOH}), 1640 (s, $\nu_{CH=N}$). ^1H NMR data (d-DMSO, ppm): $\delta = 1.41$ (s, 3H, CH_3), 3.61 (br, 2H, CH_2OH), 3.81 (s, 4H, CH_2OH), 6.90–7.62 (m, 3H, aromatic), 8.51 (s, 1H, CH=N), 13.1 (s, 1H, ArO*H*). UV-Vis (λ, nm): 261, 392.

2.3. *Synthesis of HL^2 and HL^3*

The yellow microcrystalline products of HL^2 and HL^3 were prepared by the same method as described for HL^1, with similar starting materials. Yields: 93% for HL^2 and 87% for HL^3. For HL^2: Anal. Calcd for $C_{13}H_{19}NO_4$ (%): C, 61.6; H, 7.6; N, 5.5. Found: C, 61.3; H, 7.6; N, 5.6. IR data (KBr, cm^{-1}): 3327 (br, w, ν_{ArOH}), 1637 (s, $\nu_{CH=N}$). ^1H NMR data (d-DMSO, ppm): $\delta = 0.89$ (t, 3H, CH_2CH_3), 1.60 (q, 2H, CH_2CH_3), 3.62 (br, 2H, CH_2OH), 3.81 (s, 4H, CH_2OH), 3.85 (s, 3H, OCH_3), 6.83–7.26 (m, 3H, aromatic), 8.51 (s, 1H, CH=N), 12.8 (s, 1H, ArO*H*). UV-Vis (λ, nm): 263, 396. For HL^3: Anal. Calcd for $C_{11}H_{14}BrNO_3$ (%): C, 45.8; H, 4.9; N, 4.9. Found: C, 45.6; H, 5.0; N, 4.7. IR data (KBr, cm^{-1}): 3313 (br, w, ν_{ArOH}), 1641 (s, $\nu_{CH=N}$). ^1H NMR data (d-DMSO, ppm): $\delta = 1.41$ (s, 3H, CH_3), 3.61 (br, 2H, CH_2OH), 3.81 (s, 4H, CH_2OH), 6.80–7.81 (m, 3H, aromatic), 8.51 (s, 1H, CH=N), 12.7 (s, 1H, ArO*H*). UV-Vis (λ, nm): 262, 395.

2.4. *Synthesis of $[Zn(L^1)_2]\cdot H_2O$ (1)*

To methanolic solution (10 cm^3) of HL^1 (48.6 mg, 0.2 mmol) was added an aqueous solution (3 cm^3) of $Zn(ClO_4)_2\cdot 6H_2O$ (37.2 mg, 0.1 mmol) with stirring. The mixture was stirred for 30 min at room temperature to give a clear colorless solution. After keeping the solution in air for a few days, small colorless block-shaped crystals of the complex, suitable for X-ray crystal structural determination, formed at the bottom of the vessel on slow evaporation of the solvent. The crystals were isolated, washed three times with cold water/methanol (V : V = 1 : 1), and dried in a vacuum desiccator containing anhydrous $CaCl_2$. Yield: 27 mg, 47% (based on HL^1). Anal. Calcd for $C_{22}H_{28}Cl_2N_2O_7Zn$ (%): C, 46.5; H, 5.0; N, 4.9. Found: C, 46.3; H, 5.0; N, 4.9. IR data (KBr, cm^{-1}): 3403 (br, w, ν_{water}), 3272 (w, ν_{OH}), 1631 (s, $\nu_{CH=N}$). UV-Vis (λ, nm): 246, 373, 580.

2.5. *Synthesis of $[Ni(L^1)_2]\cdot H_2O$ (2), $[Ni(L^2)_2]$ (3), and $[Co(L^3)_2]\cdot H_2O$ (4)*

Complexes **2**, **3**, and **4** were prepared by the same method as that described for **1**, with similar starting materials. Yields: 55% for **2**, 63% for **3**, and 46% for **4**. For **2**: Anal. Calcd for $C_{22}H_{28}Cl_2N_2NiO_7$ (%): C, 47.0; H, 5.0; N, 5.0. Found: C, 46.7; H, 5.1; N, 5.0. IR data (KBr, cm^{-1}): 3391 (br, w, ν_{water}), 3273 (w, ν_{OH}), 1631 (s, $\nu_{CH=N}$). UV-Vis (λ, nm): 245, 377, 615, 963. For **3**: Anal. Calcd for $C_{26}H_{36}N_2NiO_8$ (%): C, 55.4; H, 6.4; N, 5.0. Found: C, 55.6; H, 6.6; N, 4.8. IR data (KBr, cm^{-1}): 3275 (w, ν_{OH}), 1628 (s, $\nu_{CH=N}$). UV-Vis (λ, nm): 243, 380, 610, 965. For **4**: Anal. Calcd for $C_{22}H_{28}Br_2CoN_2O_7$ (%): C, 40.6; H, 4.3; N, 4.3. Found: C, 40.3; H, 4.5; N, 4.2. IR data (KBr, cm^{-1}): 3397 (br, w, ν_{water}), 3272 (w, ν_{OH}), 1633 (s, $\nu_{CH=N}$). UV-Vis (λ, nm): 247, 380, 515.

2.6. *X-ray structural determination*

Diffraction intensities for HL^1 and the complexes were collected at 298(2) K using a Bruker SMART CCD area detector with Mo-Kα radiation (λ = 0.71073 Å). The collected data were reduced using SAINT [15] and multi-scan absorption corrections were performed using SADABS [16]. The structures were solved by direct methods and

refined against F^2 by full-matrix least-squares using the SHELXTL package [17]. All non-hydrogen atoms were refined anisotropically. The imino H in **1** and the hydroxyl and water hydrogen atoms in the complexes were located in difference Fourier maps and refined isotropically with N–H, O–H, and H···H distances restrained to 0.90(1), 0.85(1), and 1.37(2) Å, respectively. All other hydrogen atoms were placed in geometrically ideal positions and constrained to ride on their parent atoms. The crystallographic data for the compounds are summarized in table 1. Selected bond lengths and angles are given in table 2.

2.7. *Urease inhibitory activity assay*

Helicobacter pylori (ATCC 43504; American Type Culture Collection, Manassas, VA) was grown in brucella broth supplemented with 10% heat-inactivated horse serum for 24 h at 37°C under microaerobic conditions (5% O_2, 10% CO_2, and 85% N_2). The method of preparation of the urease by Mao *et al.* [18] was followed. Briefly, broth cultures (50 mL, 2.0×10^8 CFU mL^{-1}) were centrifuged (5000 *g*, 4°C) to collect the bacteria, and after washing twice with phosphate-buffered saline (pH = 7.4), the *H. pylori* precipitate was stored at −80°C. While the *H. pylori* was returned to room temperature, and mixed with 3 mL of distilled water and protease inhibitors, sonication was performed for 60 s. Following centrifugation (15,000 *g*, 4°C), the supernatant was desalted through SephadexG–25 column (PD–10 columns, Amersham–Pharmacia Biotech, Uppsala, Sweden). The resultant crude urease solution was added to an equal volume of glycerol and stored at 4°C until use in the experiment. The mixture, containing 25 μL (4U) of the urease and 25 μL of the test compound, was pre-incubated for 3 h at room temperature in a 96-well assay plate. Urease activity was determined for three parallel times by measuring ammonia production using the indophenol method as described by Weatherburn [19].

2.8. *Molecular docking study*

Molecular docking of the complexes into the 3-D X-ray structure of the *H. pylori* urease (entry 1E9Y in the Protein Data Bank) was carried out by using AutoDock 4.2 software as implemented through the graphical user interface AutoDockTools (ADT 1.5.4). The graphical user interface AutoDockTools was employed to setup the enzymes: all hydrogen atoms were added, Gasteiger charges were calculated and non-polar hydrogen atoms were merged to carbons. The Ni initial parameters are set as $r = 1.170$ Å, $q = +2.0$, and van der Waals well depth of 0.100 $kcalmol^{-1}$ [20]. The molecules of the compounds were transferred to pdb files with the program ChemBio3D. The pdb files were further transferred to pdbqt files with the AutoDockTools.

AutoDockTools was used to generate the docking input files. In the docking grid box sizes of $40 \times 50 \times 40$ for HL^1 and $70 \times 60 \times 60$ for the complexes points in *x*, *y*, and *z* directions were built, the maps were centered on the original ligand molecule in the active site of the protein. A grid spacing of 0.375 Å and a distances-dependent function of the dielectric constant were used for the calculation of the energy map. 100 runs were generated by using Lamarckian genetic algorithm searches. Default settings were used with an initial population of 50 randomly placed individuals, a maximum number of

Table 1. Crystallographic and experimental data for HL^1 and **1–4**.

Compound	HL^1	**1**	**2**	**3**	**4**
Empirical formula	$C_{11}H_{14}ClNO_3$	$C_{22}H_{28}Cl_2N_2O_7Zn$	$C_{22}H_{28}Cl_2N_2NiO_7$	$C_{26}H_{36}N_2NiO_8$	$C_{22}H_{28}Br_2CoN_2O_7$
Formula weight	243.7	568.7	562.1	563.3	651.2
Temperature (K)	298(2)	298(2)	298(2)	298(2)	298(2)
Crystal shape/color	Block/yellow	Block/colorless	Block/green	Block/green	Block/red
Crystal system	Orthorhombic	Monoclinic	Monoclinic	Triclinic	Monoclinic
Space group	$P2_12_12_1$	$C2/c$	$C2/c$	P-1	$C2/c$
Unit cell dimensions (Å, °)					
a	5.993(2)	28.955(2)	28.965(3)	10.922(1)	29.038(3)
b	8.833(2)	11.676(2)	11.624(3)	11.550(1)	11.622(1)
c	21.537(3)	18.225(3)	18.336(3)	12.775(2)	18.441(2)
α	90	90	90	99.087(2)	90
β	90	125.942(3)	126.822(2)	106.891(2)	124.583(1)
γ	90	90	90	112.495(1)	90
V (Å^3), Z	1140.1(5), 4	4988.4(12), 8	4941.9(16), 8	1357.1(3), 2	5123.8(10), 8
Calculated density (g cm^{-3})	1.420	1.515	1.511	1.378	1.688
μ(Mo-Kα) (cm^{-1})	0.326	1.243	1.046	0.765	3.833
F(000)	512	2352	2336	596	2616
Crystal size (mm^3)	0.30×0.27×0.23	0.23×0.21×0.20	0.18×0.17×0.13	0.32×0.27×0.27	0.17×0.13×0.13
R_{int}	0.0317	0.0554	0.1053	0.0156	0.0752
Measured reflections	6773	13,191	12,006	7937	12,812
Unique reflections	2473	5367	5313	5721	4681
Observed reflections [$I \geq 2\sigma(I)$]	2041	3427	2448	4745	2593
Parameters/restraints	151/1	323/5	323/5	346/2	323/5
Min./max. transmission	0.9084/0.9287	0.7630/0.7891	0.8340/0.8760	0.7919/0.8201	0.5619/0.6357
Goodness-of-fit on F^2	1.038	1.006	0.973	1.013	0.962
R_1, wR_2 [$I \geq 2\sigma(I)$][a]	0.0390, 0.0754	0.0505, 0.1044	0.0812, 0.1718	0.0351, 0.0814	0.0524, 0.0911
R_1, wR_2 (all data)[a]	0.0519, 0.0803	0.0935, 0.1200	0.1772, 0.2266	0.0456, 0.0875	0.1204, 0.1121

[a] $R_1 = \sum||F_o| - |F_c||/\sum|F_o|$, $wR_2 = \left[\sum w(F_o^2 - F_c^2)^2/\sum w(F_o^2)^2\right]^{1/2}$.

Table 2. Selected bond lengths (Å) for HL^1 and **1–4**.

HL^1			
N1–C7	1.296(3)	N1–C8	1.485(3)
O1–C2	1.292(2)	O2–C9	1.416(2)
O3–C10	1.413(3)		
1			
Zn1–O1	2.056(2)	Zn1–O2	2.251(3)
Zn1–O4	2.017(2)	Zn1–O5	2.280(3)
Zn1–N1	2.082(3)	Zn1–N2	2.075(3)
2			
Ni1–O1	2.019(4)	Ni1–O2	2.129(5)
Ni1–O4	2.038(4)	Ni1–O6	2.158(5)
Ni1–N1	2.028(5)	Ni1–N2	2.042(5)
3			
Ni1–O1	1.986(1)	Ni1–O3	2.097(1)
Ni1–O5	1.991(1)	Ni1–O7	2.099(1)
Ni1–N1	2.010(2)	Ni1–N2	2.009(2)
4			
Co1–O1	2.045(3)	Co1–O3	2.175(4)
Co1–O4	2.017(4)	Co1–O6	2.160(4)
Co1–N1	2.081(4)	Co1–N2	2.089(4)

2.5×10^6 energy evaluations, and a maximum number of 2.7×10^4 generations. A mutation rate of 0.02 and a crossover rate of 0.8 were chosen. The results of the most favorable free energy of binding were selected as the resultant complex structures.

3. Results and discussion

3.1. *Chemistry*

The Schiff bases HL^1, HL^2, and HL^3 were obtained as yellow solid products, stable in air at room temperature, and soluble in common polar organic solvents such as DMSO, DMF, methanol, ethanol, and acetonitrile. Single-crystals suitable for X-ray diffraction for HL^1 were obtained; however, for HL^2 and HL^3 it is hard to obtain well-shaped single-crystals from common organic solvents, including methanol, ethanol, dichloromethane, and acetonitrile. The complexes derived from the Schiff bases were all crystallized as mononuclear compounds. They are also stable in air at room temperature, soluble in DMF, DMSO, and acetonitrile, but slightly soluble in methanol and ethanol, and insoluble in water. The molar conductivities of the complexes measured in acetonitrile at 10^{-3} mol L^{-1} are 10–25 Ω^{-1} cm^2 mol^{-1}, indicating the non-electrolytic nature of the complexes in solution [21].

3.2. *IR spectra*

IR spectra of the Schiff bases and their complexes provide information about the metal–ligand bonding. Assignments are based on typical group frequencies. Weak and broad absorptions centered at 3313–3327 cm^{-1} in spectra of the Schiff bases and at 3273 cm^{-1} in the complexes are attributed to hydroxyl groups. The weak and broad absorption

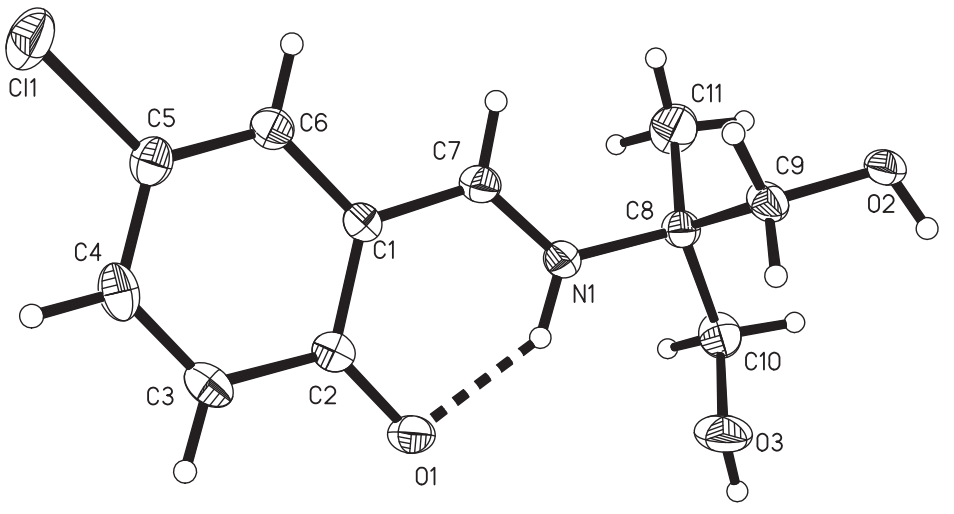

Figure 1. The structure of HL^1 showing the atom-numbering scheme. Displacement ellipsoids are drawn at the 30% probability level and hydrogen atoms are shown as small spheres of arbitrary radii. Intramolecular hydrogen bond is shown as a dashed line.

centered at 3400 cm^{-1} in spectra of **1**, **2**, and **4** are attributed to lattice water molecules. Several weak peaks observed for HL^1 and the complexes from 3180 to 2860 cm^{-1} are due to the aromatic and aliphatic C–H stretches. Strong absorptions at 1640 cm^{-1} in spectra of the Schiff bases are assigned to azomethine, ν(C=N) [22]. These bands shift to lower wavenumbers in the complexes (1628–1633 cm^{-1}), attributed to coordination of nitrogen of the azomethine to metal. The phenolic ν(Ar–O) in the Schiff bases exhibit strong bands at 1230 cm^{-1} [23]. However, in the complexes the bands appear at 1165–1183 cm^{-1}, which may be assigned to skeletal vibration related to phenolic oxygen, shifted to lower frequencies when the phenolic oxygen atoms coordinate [24, 25]. The weak bands at 410–550 cm^{-1} for the complexes can be assigned to the M–O and M–N vibrations [26].

The close resemblance of the shape and the positions of the absorption bands suggest similar coordination modes for the complexes. IR spectra of HL^1 and the complexes are consistent with the X-ray structural results.

3.3. *Structures of HL^1 and the complexes*

Figures 1–5 give perspective views of HL^1 and **1**–**4** with atomic labeling systems. In the molecular structure of HL^1, hydrogen of hydroxyl is transferred to the imino nitrogen, generating an intramolecular N1–H1 $\cdots$ O1 hydrogen bond. The formation of the N–H bond made the C7–N1 bond slightly longer than typical C=N bonds. Complexes **1**, **2**, **3**, and **4** are structurally similar mononuclear zinc(II), nickel(II), nickel(II), and cobalt(II) compounds, respectively. Complexes **1**, **2**, and **4** contain a water of crystallization. Zn, Ni, and Co in the complexes are six-coordinate by two imino nitrogen atoms, two phenolate oxygen atoms, and two hydroxyl oxygen atoms from two deprotonated Schiff-base ligands, forming distorted octahedral geometry. The distortion of the

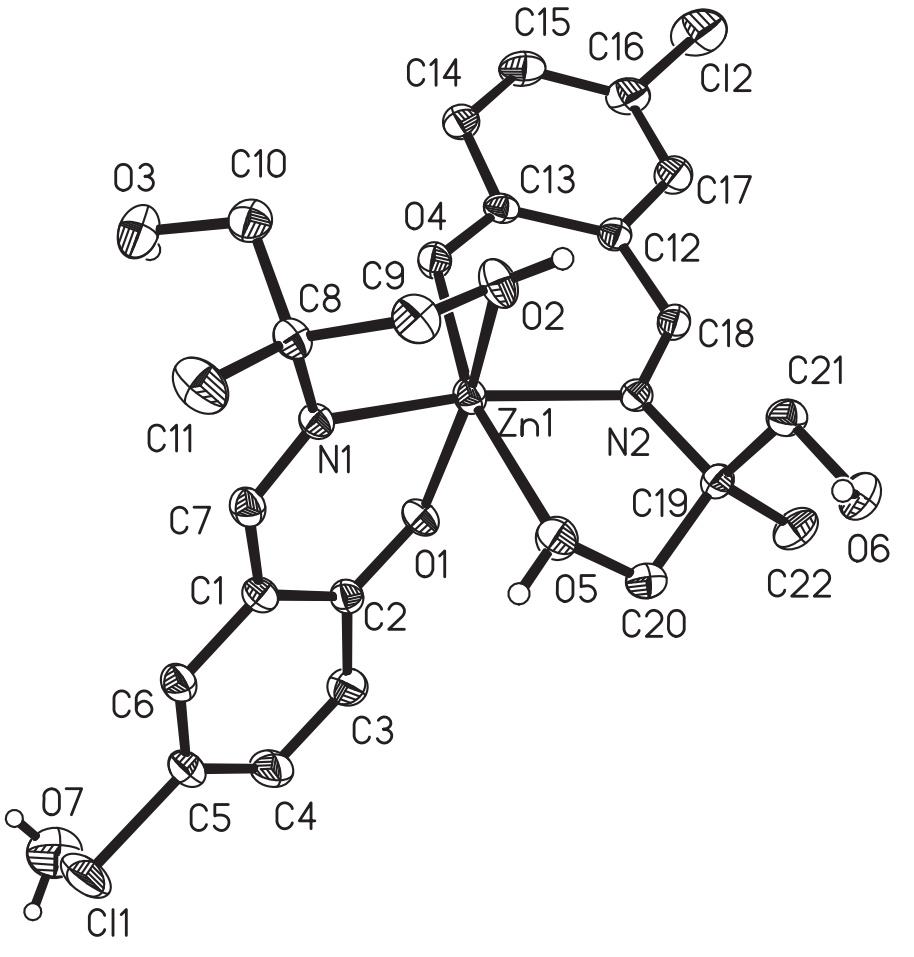

Figure 2. The structure of **1** showing the atom-numbering scheme. Displacement ellipsoids are drawn at the 30% probability level.

octahedral coordination can be observed from the bond angles subtended at the metal, ranging from 76.3(1) to 103.2(1)° for **1**, 78.2(2) to 98.8(2)° for **2**, 81.8(1) to 95.2(1)° for **3**, and 76.8(2) to 100.5(2)° for **4** for the perpendicular angles, and from 163.8(1) to 166.1(1)° for **1**, 168.0(2) to 170.7(2)° for **2**, 171.1(1) to 175.8(1)° for **3**, and 165.4(1) to 168.0(2)° for **4** for the longitudinal angles. The two Schiff-base ligands in the complexes are almost perpendicular to each other, decreasing the steric effects between the molecules. The dihedral angles between the two benzene rings are 69.5(2)° for **1**, 66.1(2)° for **2**, 84.2(2)° for **3**, and 71.8(3)° for **4**.

The Schiff-base ligands coordinate to metal as the deprotonated form. The bond lengths of C7–N1 and C18–N2 in **1** and **2** are shorter than that of C7–N1 in HL[1], together with the bond lengths of C2–O1 and C13–O4 in **1** and **2** being longer than that of C2–O1 in HL[1], indicating the coordination of the imino N and the phenolate O. For the C–O bonds of the propane-1,3-diol moiety, there are no obvious changes during coordination.

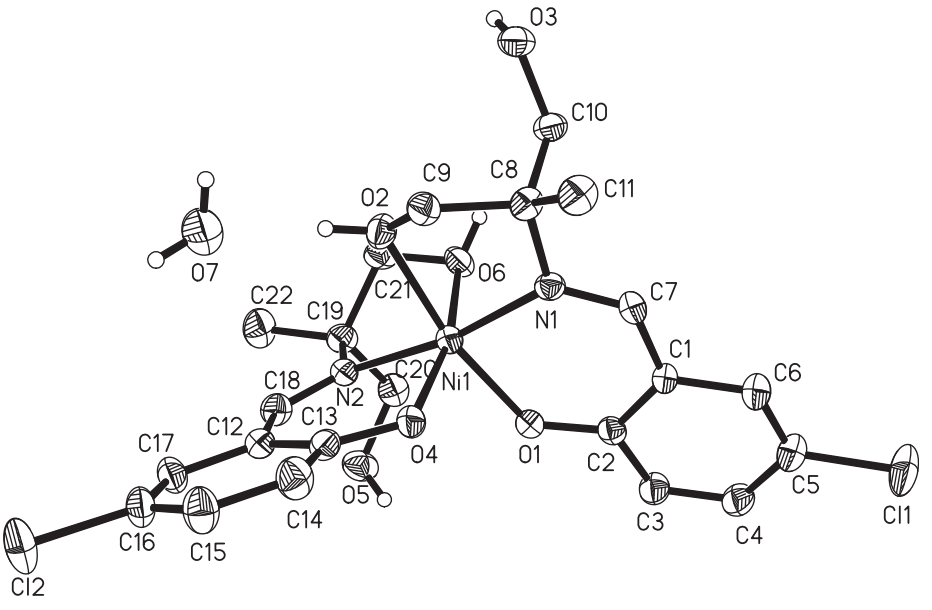

Figure 3. The structure of **2** showing the atom-numbering scheme. Displacement ellipsoids are drawn at the 30% probability level.

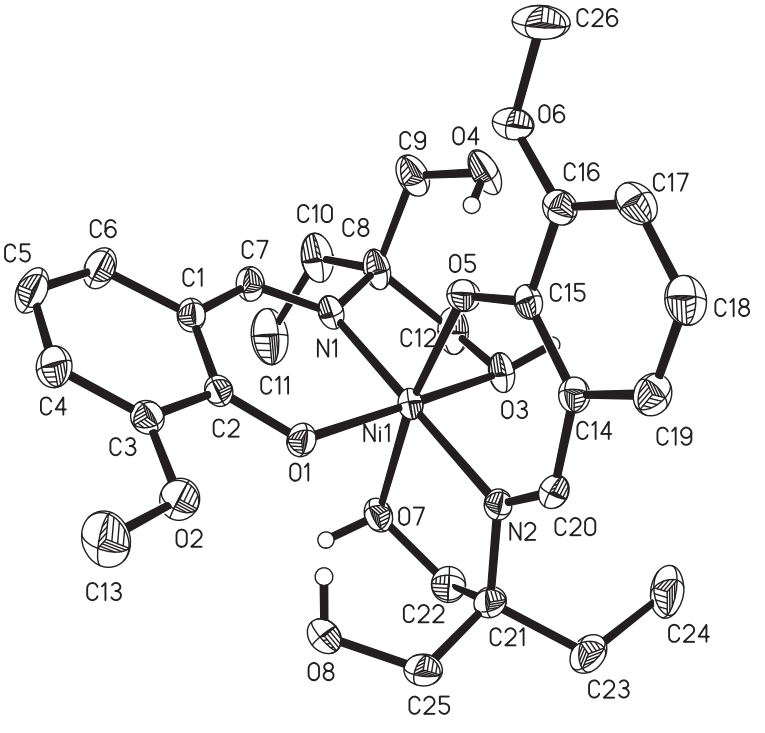

Figure 4. The structure of **3** showing the atom-numbering scheme. Displacement ellipsoids are drawn at the 30% probability level.

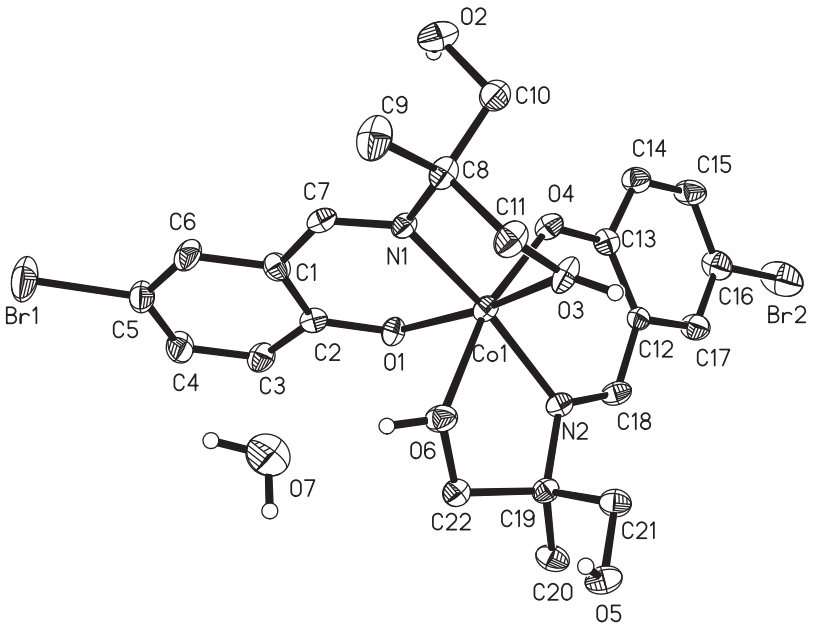

Figure 5. The structure of **4** showing the atom-numbering scheme. Displacement ellipsoids are drawn at the 30% probability level.

Table 3. Geometrical parameters for hydrogen bonds.

Hydrogen bonds	D–H (Å)	H···A (Å)	D···A (Å)	D–H···A (°)
HL[1]				
N1–H1···O1	0.91(1)	1.82(2)	2.602(2)	142(3)
O3–H3···O2$^{\#1}$	0.82	1.91	2.677(2)	156
O2–H2···O1$^{\#2}$	0.82	1.83	2.645(2)	174
1				
O3–H3···O6$^{\#3}$	0.82	1.96	2.749(4)	160
O6–H6···O4$^{\#4}$	0.82	1.91	2.697(3)	160
O2–H2···O1$^{\#4}$	0.85(1)	1.79(1)	2.628(3)	168(5)
O5–H5···O7$^{\#5}$	0.84(1)	1.96(2)	2.769(5)	162(5)
2				
O3–H3···O1$^{\#4}$	0.82	1.90	2.671(6)	157
O6–H6···O4$^{\#4}$	0.85(1)	1.80(3)	2.628(6)	165(8)
O5–H5···O3$^{\#3}$	0.82	1.95	2.745(7)	163
O2–H2···O7	0.85(1)	1.88(2)	2.724(8)	172(8)
3				
O4–H4···O5	0.82	1.84	2.651(2)	169
O8–H8···O1	0.82	1.86	2.657(2)	163
O7–H7···O8$^{\#6}$	0.84(1)	1.85(1)	2.679(2)	168(3)
O3–H3···O4$^{\#7}$	0.84(1)	1.86(1)	2.667(2)	161(3)
4				
O2–H2···O5$^{\#3}$	0.82	1.92	2.720(5)	163
O5–H5···O4$^{\#4}$	0.82	1.97	2.699(5)	148
O3–H3···O1$^{\#4}$	0.85(1)	1.80(1)	2.647(5)	175(6)
O6–H6···O7	0.85(1)	1.86(1)	2.712(7)	174(7)
O7–H7A···O2$^{\#8}$	0.85(1)	1.94(2)	2.760(6)	162(7)

Symmetry codes: $^{\#1}$ $1+x, y, z$; $^{\#2}$ $1-x, -1/2+y, 3/2-z$; $^{\#3}$ $1/2-x, -1/2+y, 1/2-z$; $^{\#4}$ $1/2-x, 1/2+y, 1/2-z$; $^{\#5}$ $x, 1+y, z$; $^{\#6}$ $1-x, 1-y, 2-z$; $^{\#7}$ $-x, -y, 1-z$; $^{\#8}$ $x, 2-y, 1/2+z$.

Table 4. Inhibition of urease by the tested materials.

Tested materials	Inhibition rate* (%)
HL^1	83 ± 3
1	40 ± 2
2	43 ± 3
3	38 ± 2
4	33 ± 2
Acetohydroxamic acid	90 ± 4

*The concentration of the tested material is 100 μmol L^{-1}.

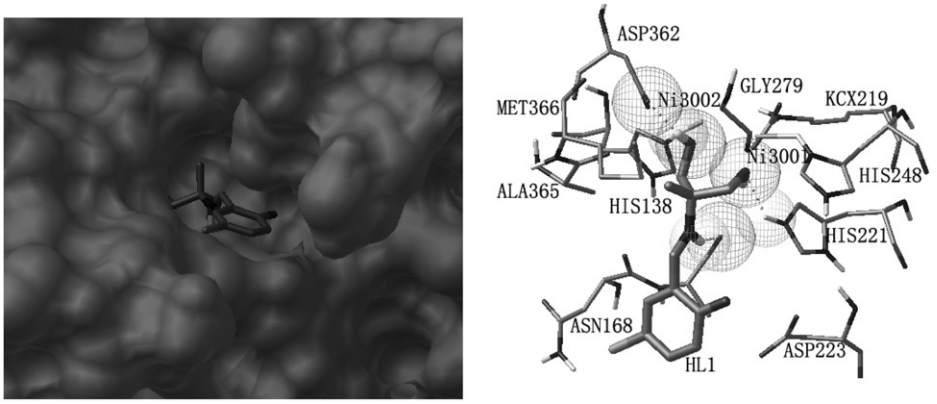

Figure 6. Binding mode of HL^1 with *H. pylori* urease. Left: the enzyme is shown as surface and HL^1 is shown as sticks. Right: hydrogen bonds are shown as dashed lines.

In the crystal structures of HL^1 and the complexes, molecules are linked through intermolecular O–H $\cdots$ O hydrogen bonds (table 3), forming 1-D chains.

3.4. *Pharmacology*

The results of the urease inhibition are given table 4. The acetohydroxamic acid (AHA) was used as a reference. HL^1 exhibits effective activity and the complexes show relatively weak activities. Considering that the structures of the complexes are very similar to each other, the central metals play no role during the inhibition.

3.5. *Molecular docking study*

The molecular docking study was performed to investigate the binding interactions between the compounds and the active site of the *H. pylori* urease. In the X-ray structure available for native urease, two nickels were coordinated by *His*136, *His*138, *Kcx*219, *His*248, *His*274, *Asp*362, and water, while in the AHA-inhibited urease, the water molecules were replaced by AHA [27]. In order to give an explanation on the inhibitory activity of the compounds, molecular docking of the compounds into the

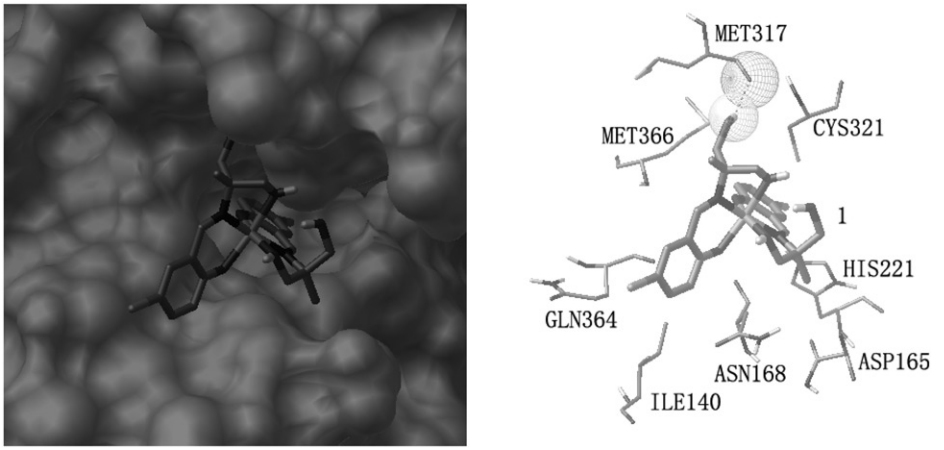

Figure 7. Binding mode of **1** with *H. pylori* urease. Left: the enzyme is shown as surface and **1** is shown as sticks. Right: hydrogen bonds are shown as dashed lines.

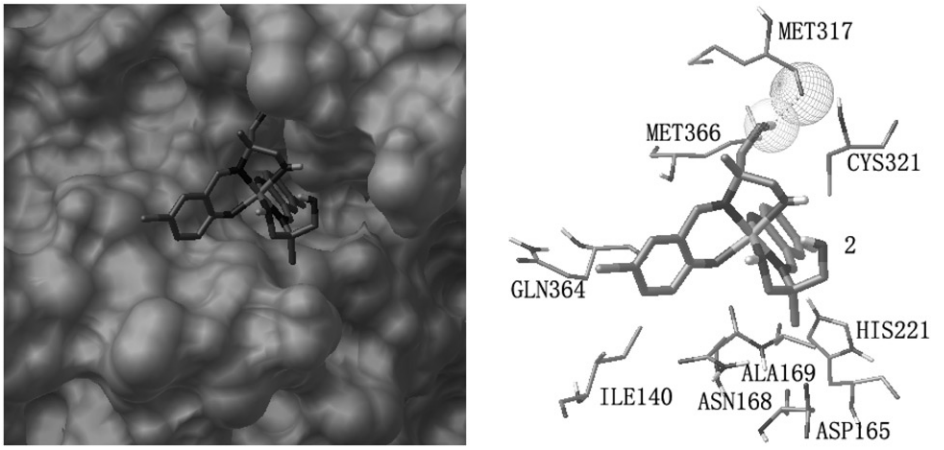

Figure 8. Binding mode of **2** with *H. pylori* urease. Left: the enzyme is shown as surface and **2** is shown as sticks. Right: hydrogen bonds are shown as dashed lines.

AHA binding site of the urease was performed on the binding model based on the urease complex structure (1E9Y.pdb). The binding models of the compounds and the urease are depicted in figures 6–10. HL^1 is well filled in the active pocket of the urease, with docking score of −7.31. Four hydrogen bonds form between HL^1 and the urease. In addition, two hydroxyl groups of HL^1 are very close to the two Ni's of the active site of urease. For **1**, **2**, **3**, and **4** the docking scores are −6.36, −6.37, −5.43, and −6.61, respectively. Even though they are lower than the docking score of AHA (−5.01), they show only weak inhibitory activities. This might be caused by the large bulk of the complex molecules, which made them difficult to approach the active site of the urease. The complex molecules are located at the entry of the pocket, leading to urea molecules difficulty binding with the active site of the urease. This might explain why the

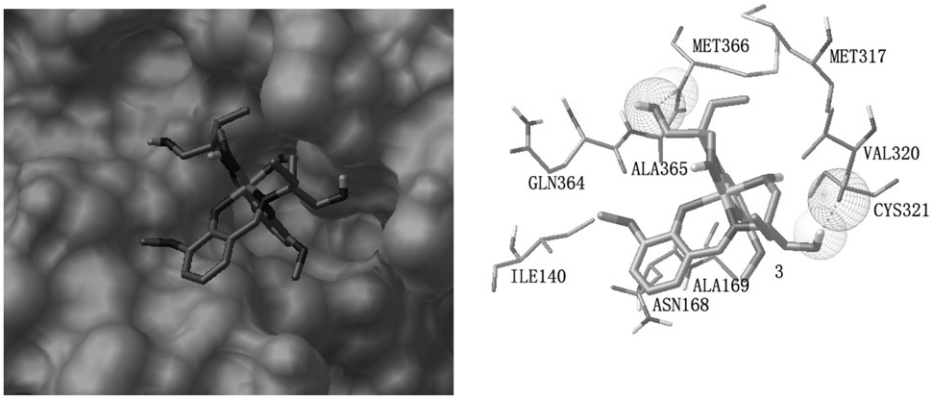

Figure 9. Binding mode of **3** with *H. pylori* urease. Left: the enzyme is shown as surface and **3** is shown as sticks. Right: hydrogen bonds are shown as dashed lines.

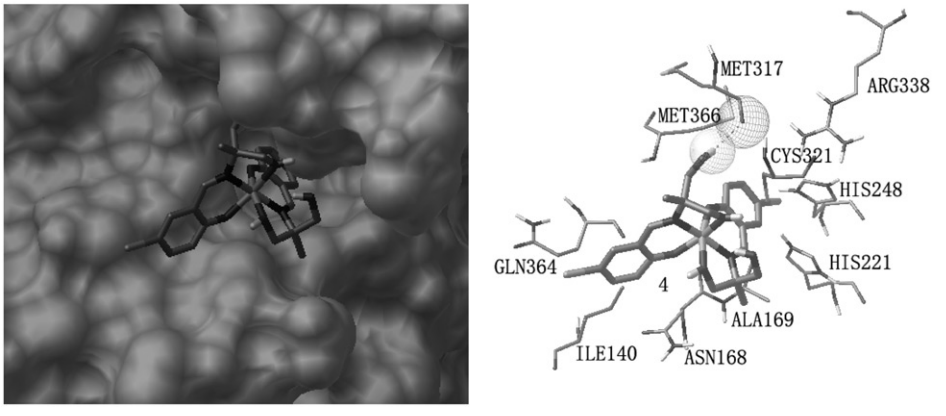

Figure 10. Binding mode of **4** with *H. pylori* urease. Left: the enzyme is shown as surface and **4** is shown as sticks. Right: hydrogen bonds are shown as dashed lines.

complexes show weak inhibitory activities. The results of the molecular docking study explain well the activities of the compounds against *H. pylori* urease.

4. Conclusion

In this work, three hydroxy-rich Schiff bases were used to prepare four new zinc(II), nickel(II), and cobalt(II) complexes. The crystal structures of the Schiff base HL^1 and the complexes were characterized by X-ray diffraction. All the reactions resulted in the formation of mononuclear complexes where the metal is bound to two mono-anionic Schiff-base ligands. The Schiff bases coordinate tridentate to the metal through phenolato O, imino N, and one hydroxyl O. The Schiff base HL^1 exhibits activity against *H. pylori* urease, while the complexes show relatively weak activities.

Supplementary material

Crystallographic data for HL^1 and the complexes have been deposited with the Cambridge Crystallographic Data Centre as supplementary publication nos. CCDC 832398 (HL^1), 832399 (**1**), 838254 (**2**), 838255 (**3**), 838256 (**4**). Copies of these data can be obtained free of charge *via* www.ccdc.cam.ac.uk/data_request/cif, by emailing data_request@ccdc.cam.ac.uk, or by contacting The Cambridge Crystallographic Data Centre, 12 Union Road, Cambridge CB21EZ, UK; Fax: +44 1223 336033.

Acknowledgments

This work was financially supported by the National Science Foundation of China (Project No. 20901036).

References

[1] R.D. Archer, B. Wang. *Inorg. Chem.*, **29**, 39 (1990).
[2] I. Bertini, H.B. Gray, S.J. Lippard, J.S. Valentine. *Bioinorganic Chemistry*, University Science Books, Mills Valley, CA, USA (1994).
[3] S.C. Bhatia, J.M. Bindlish, A.R. Saini, P.C. Jain. *J. Chem. Soc., Dalton Trans.*, 1773 (1981).
[4] S. Chang, L. Jones, C.M. Wang, L.M. Henling, R.H. Grubbs. *Organometallics*, **17**, 3460 (1998).
[5] P.S. Dixit, K. Srinivasan. *Inorg. Chem.*, **27**, 4507 (1988).
[6] D.P. Kessissoglou, W.M. Butler, V.L. Pecoraro. *Inorg. Chem.*, **26**, 495 (1987).
[7] H. Miyasaka, N. Matsumoto, H. Okawa, N. Re, E. Gallo, C. Floriani. *J. Am. Chem. Soc.*, **118**, 981 (1996).
[8] R. Ramnauth, S. Al-Juaid, M. Motevalli, B.C. Parkin, A.C. Sullivan. *Inorg. Chem.*, **43**, 4072 (2004).
[9] V. Tangoulis, D.A. Malamatari, K. Soulti, V. Stergiou, C.P. Raptopoulou, A. Terzis, T.A. Kabanos, D.P. Kessissoglou. *Inorg. Chem.*, **35**, 4974 (1996).
[10] A.N. Papadopoulos, C.P. Raptopoulos, A. Terzis, A.G. Hatzidimitriou, A. Gourdon, D.P. Kessissoglou. *J. Chem. Soc., Dalton Trans.*, 2591 (1995).
[11] P.V. Rao, C.P. Rao, A. Sreedhara, E.K. Wegelius, K. Rissanen, E. Kolehmainen. *J. Chem. Soc., Dalton Trans.*, 1213 (2000).
[12] Z.-L. You, Y.-M. Cui, Y.-P. Ma, C. Wang, X.-S. Zhou, K. Li. *Inorg. Chem. Commun.*, **14**, 636 (2011).
[13] Z.-L. You, H. Sun, B.-W. Ding, Y.-P. Ma, M. Zhang, D.-M. Xian. *J. Coord. Chem.*, **64**, 3510 (2011).
[14] Z.-L. You, L.-L. Ni, D.-H. Shi, S. Bai. *Eur. J. Med. Chem.*, **45**, 3196 (2010).
[15] Bruker. *SMART (Version 5.628) and SAINT (Version 6.02)*, Bruker AXS Inc., Madison, Wisconsin, USA (1998).
[16] G.M. Sheldrick. *SADABS. Program for Empirical Absorption Correction of Area Detector*, University of Göttingen, Germany (1996).
[17] G.M. Sheldrick. *SHELXTL V5.1 Software Reference Manual*, Bruker AXS, Inc., Madison, Wisconsin, USA (1997).
[18] W.-J. Mao, P.-C. Lv, L. Shi, H.-Q. Li, H.-L. Zhu. *Bioorg. Med. Chem.*, **17**, 7531 (2009).
[19] M.W. Weatherburn. *Anal. Chem.*, **39**, 971 (1967).
[20] B. Krajewska, W. Zaborska. *Bioorg. Chem.*, **35**, 355 (2007).
[21] W.J. Geary. *Coord. Chem. Rev.*, **7**, 81 (1971).
[22] J.E. Kovacic. *Spectrochim. Acta*, **A23**, 183 (1963).
[23] G.C. Percy, D.A. Thornton. *J. Inorg. Nucl. Chem.*, **34**, 3357 (1972).
[24] C. Fukuhara, E. Asato, T. Shimoji, K. Katsura, M. Mori, K. Matsumoto, S. Ooi. *J. Chem. Soc., Dalton Trans.*, 1305 (1987).
[25] T. Tokki, Y. Muto, K. Imai, H.B. Janassen. *J. Inorg. Nucl. Chem.*, **35**, 1539 (1973).
[26] M.M. Bekheit, K.M. Ibrahim. *Synth. React. Inorg. Met.-Org. Chem.*, **16**, 1135 (1986).
[27] Z.-P. Xiao, T.-W. Ma, W.-C. Fu, X.-C. Peng, A.-H. Zhang, H.-L. Zhu. *Eur. J. Med. Chem.*, **45**, 5064 (2010).